Preform Characterization in VARTM Process Model Development

Brian W. Grimsley[I], Roberto J. Cano[I], Pascal Hubert[II],
Alfred C. Loos[III], Charles B. Kellen[IV] and Brian J. Jensen[I]

[I] NASA Langley Research Center, Hampton, Virginia 23681
[II] McGill University, Montreal, Quebec, Canada H3A2K6
[III] Michigan State University, East Lansing, Michigan 48824
[IV] Old Dominion University, Norfolk, VA 23508

ABSTRACT [1]

Vacuum-Assisted Resin Transfer Molding (VARTM) is a Liquid Composite Molding (LCM) process where both resin injection and fiber compaction are achieved under pressures of 101.3 kPa or less. Originally developed over a decade ago for marine composite fabrication, VARTM is now considered a viable process for the fabrication of aerospace composites (1,2). In order to optimize and further improve the process, a finite element analysis (FEA) process model is being developed to include the coupled phenomenon of resin flow, preform compaction and resin cure. The model input parameters are obtained from resin and fiber-preform characterization tests. In this study, the compaction behavior and the Darcy permeability of a commercially available carbon fabric are characterized. The resulting empirical model equations are input to the 3-Dimensional Infiltration, version 5 (3DINFILv.5) process model to simulate infiltration of a composite panel.

KEY WORDS: Vacuum-Assisted RTM, Characterization, Finite Element Analysis

1.0 INTRODUCTION

Unlike other LCM processes such as resin transfer molding (RTM), the VARTM process allows fabrication of composite parts without the use of any supplied pressure. Both transfer of the matrix resin and compaction of the part are achieved using atmospheric pressure alone. Therefore, the upper tool of the matched metal mold used in RTM is replaced in the VARTM

process by a formable vacuum bag material. Flow of the resin into the part is enhanced through the use of a resin distribution medium (3,4). The highly-permeable medium induces resin flow through the thickness of the part and reduces filling times.

Work under the Twenty-First Century Aircraft Technology (TCAT) program at NASA Langley Research Center has focused on further developing the VARTM process for fabrication of composite structures for high-performance aircraft. The development and use of a finite element process model is an important part of this research. The process model allows sensitivity analyses to determine the influence of intrinsic (e.g. constitutive material properties) and extrinsic (e.g. cure cycle) parameters on the final part quality (5). In addition, a model which accurately predicts infiltration, cure and final part dimensions greatly reduces the cost associated with the trial and error procedure commonly used in manufacturing to develop a suitable processing cycle.

The process model 3DINFIL predicts three-dimensional flow evolution, part injection times, and final part dimensions using a finite element/control volume technique (6). Previously developed for RTM, the 3DINFIL model has been modified for application to the VARTM process by coupling the flow sub-model to a compaction sub-model (6). This is critical to accurately predicting the particular resin flow behavior caused by the presence of a flexible bag and low compaction pressures found in the VARTM process. The key material input properties required by the model are the preform compaction behavior and the permeability. These two properties are coupled by the state of the preform, such as the fiber volume fraction and the saturation. In this work, the compaction and permeability of a preform specimen containing four stacks of the SAERTEX®[2] multi-axial, warp-knit (MAWK) carbon fabric preforms were characterized for the range of fiber volume fractions found in typical VARTM conditions. The resulting empirical equations were used as material input parameters in 3DINFIL to simulate the flow front evolution in a four-stack, 30.5 cm x 61.0 cm flat composite panel. The results of the simulation are compared with flow front measurements obtained from infiltration experiments using a glass tool.

2.0 BACKGROUND

Previous work at NASA LaRC and by others (7-9) has led to a better understanding of the unique compaction phenomena associated with the VARTM process. In VARTM, the following equation accounts for the transverse equilibrium inside the mold cavity during impregnation:

$$P_{ATM} = P_R + P_F \qquad [1]$$

where P_{ATM} is the applied atmospheric pressure, P_R is the resin pressure and P_F is the fiber pressure (pressure supported by the preform). In the dry condition, the preform essentially supports the external pressure, $P_F = P_{ATM}$, and a dry maximum debulking deformation of the preform is reached. During infiltration, two deformation mechanisms are present in the wet area of the preform: the wetting compaction and the spring-back. The wetting compaction is caused

[2] Use of trade names or manufacturers does not constitute an official endorsement, either expressed or implied, by the National Aeronautics and Space Administration.

by a change of the arrangement or state of the fiber network, which is created by the lubrication effect of the wetting fluid. Under a given external pressure, the lubrication of the dry preform causes an increase in the preform compaction by an additional amount of wetting deformation. In VARTM, this phase typically takes place at high fiber pressure ($P_F \approx P_{ATM}$) and low resin pressure ($P_R \approx 0$). The preform spring-back mechanism occurs when the local resin pressure increases. According to Equation 1, the fiber pressure must decrease when the resin pressure increases. Consequently, the preform compaction decreases by an amount of spring-back deformation due to the reduced pressure carried by the preform. The deformation experienced during spring-back has been shown to include both elastic and time-dependent, viscoelastic recovery (10). The curves also exhibit a permanent deformation due to nesting of the fabric. At any time during the infiltration process, the net compaction of the preform depends on the relative magnitude of the wetting and the spring-back deformation mechanisms. Other work (11) to characterize the compaction of non-crimp, knitted carbon fabrics has shown that the fiber volume of the specimens at pressures ranging from 50 kPa to 700 kPa was influenced by the number of layers or "stacks" of the knitted performs in the specimen. It was found that the amount of nesting that occurs increases with the amount of stacks in a specimen. The evidence of this inter-stack influence on fiber volume would require both compaction and permeability characterization specific to the stacking sequence and thickness of the preform to be infused.

Flow of resin through fibrous media can be modeled using Darcy's law (12, 13). Modeling the flow in the VARTM process differs from the traditional RTM process. The flexible vacuum bag and varying pressure inside the mold cavity, result in a variation of the preform thickness and, hence, the fiber volume fraction of the preform during the impregnation process. As explained above, the variation of compaction pressure during infiltration necessitates measurement of the preform permeability at varying fiber volumes. Permeability is defined as the resistance to flow through porous media and is often related to the porosity using an empirical model. The three-dimensional form of Darcy's Law for an anisotropic material is written as:

$$\begin{bmatrix} \bar{q}_x \\ \bar{q}_y \\ \bar{q}_z \end{bmatrix} = \frac{1}{\eta} \begin{bmatrix} S_{xx} & S_{xy} & S_{xz} \\ S_{xy} & S_{yy} & S_{yz} \\ S_{xz} & S_{yz} & S_{zz} \end{bmatrix} \begin{bmatrix} \partial P / \partial x \\ \partial P / \partial y \\ \partial P / \partial z \end{bmatrix} \qquad [2]$$

where S_{ij} are the components of the permeability tensor, q_i are the components of the superficial velocity vector, η is the viscosity of the fluid and P is the pressure. For preform architectures that are orthotropic, the components S_{xy}, S_{xz} and S_{yz} are zero and Equation [2] simplifies to:

$$\begin{aligned} \bar{q}_x &= \frac{1}{\eta} S_{xx} \frac{\partial P}{\partial x} \\ \bar{q}_y &= \frac{1}{\eta} S_{yy} \frac{\partial P}{\partial y} \\ \bar{q}_z &= \frac{1}{\eta} S_{zz} \frac{\partial P}{\partial z} \end{aligned} \qquad [3]$$

In this work, the x-direction runs parallel to the advancing flow front in a VARTM panel infiltration. The y-direction is 90° and in-plane to x. The z-direction is the transverse, or through-thickness flow direction.

3.0 MATERIALS

The carbon fabric studied in this work is a multi-axial warp-knit (MAWK) fabric supplied by SAERTEX®. The material is composed of seven plies of both AS-4 and IM-7 carbon fibers with a total areal weight of of 1423 g/m^2. The plies are stacked, not woven, and then knitted with an alternating polyester tricot/chain knit thread in the stacking sequence described in Table 1. In this study, the 0° fiber tows were in the fabric x-direction. A fiber density of 1.78 g/cc was used for both the biaxial and MAWK fabrics.

Table 1 Ply Stacking Sequence in SAERTEX MAWK Fabric.

Ply Number	Yarn Material	Yarn Orientation	Areal Weight g/m^2
1	3K-AS4	+45°	156
2	3K-AS4	-45°	156
3	12K-IM7	0°	314
4	6K-AS4	90°	171
5	12K-IM7	0°	314
6	3K-AS4	+45°	156
7	3K-AS4	-45°	156

The wetting fluid used in the experiments was an SAE 40 motor oil supplied by Valvoline. The fluid was chosen for its relative ease of use, safe handling and low cost. The temperature of the oil during permeability and compaction experiments varied from day to day depending on the room temperature. Prior to each test the viscosity was measured using a Brookfield viscometer. For oil temperatures ranging from 21.4°C to 25.4°C, the Brookfield viscosity varied from 0.34 Pa•s to 0.24 Pa•s, respectively.

4.0 EXPERIMENTAL

Compaction and permeability characterization experiments were carried out on specimens containing four stacks of the MAWK fabric. Both, in-plane, S_{xx} and S_{yy}, and through-the-thickness, S_{zz}, permeability constants were determined for fiber volume fractions ranging from 45% to 58%.

4.1 Compaction In previous work (14), difficulties were encountered in accurately determining the initial thickness of the preform specimens. The initial thickness is a key parameter in formulating the compaction model and therefore in accurate flow predictions. In an effort to solve this problem a separate approach was taken to determine the initial “uncompacted”

thickness as well as a starting thickness at some predetermined pressure. To accomplish this, a SATEC® T1000 test frame with a TRANSDUCER TECHNIQUES® $2.2x10^{-2}$ kN load cell was utilized. The fixture consisted of two circular parallel plates with a diameter of 1.60 cm and 10.1 cm for the top and bottom plate respectively. After zeroing the fixture, a 2.54 cm x 2.54 cm specimen was placed between the two plates. The fixture was closed until the slightest load was registered, i.e. less than $2.2x10^{-3}$ N. The test was then started when the specimen was loaded at a strain rate of $1.3x10^{-3}$ mm/sec until the load reached the predetermined loading point, in this case 0.334 N which corresponds to 1.70 kPa (0.5 in Hg). At this point the strain rate was decreased to $1.3x10^{-4}$ mm/sec to allow for the viscoelastic response in the fabric. The strain rate was cycled at these rates between 0.311 N and 0.334 N until the load overcame the relaxation and continued to increase above the 0.334 N limit. Cycling the strain rate between the upper and lower bounds of load simulated a pressure hold at 1.70 kPa inside the vacuum bag. The thickness measured at this stage was used as the initial preform thickness for the fiber volume fraction calculation. The remainder of the dry compaction curve was obtained by compressing the specimen in a vacuum bag.

The vacuum bag compaction experiments were conducted in both dry and wet conditions to develop an understanding of the compaction response of the MAWK fabric at the low pressures experienced during VARTM processing. An instrumented aluminum tool was used to measure pressure and displacement of the preform. As described in previous work (7), pressure sensors (Omega Engineering, Inc., Series PX102) were mounted at the tool surface beneath the fiber preform. Linear Variable Displacement Transducers (LVDT, Omega Engineering, Inc., Series 400) were supported above the vacuum-bagged preform by a rigid beam. Sensor outputs were recorded by a PC-based data acquisition system using LabVIEW® software.

The preform specimens were carefully cut into 15 cm x 27 cm rectangles, weighed and placed on the tool. For the sake of continuity, the compaction specimens were laid-up on the tool and bagged similar to a conventional VARTM infiltration. The distribution medium, containing three layers of nylon mesh screen, was placed beneath the resin inlet distribution tubing and atop the preform to a point within 2.54 cm of the LVDT and pressure sensor. Therfore, the thickness of the media was not included in calculation of the resulting curves. The specimens were placed on the tool surface so that the advancing flow front would contact the pressure sensor at the same time that the preform under the LVDT was wetted. For the dry preform tests, the bagged preform was evacuated via one port located approximately 12 cm from the preform. The displacement was recorded at preset pressure levels from 1.70 kPa to 101 kPa after allowing the displacement to reach steady state at each of these compaction levels (approximately 200 seconds). In the wet compaction test, the resin and vacuum lines were placed following the procedure for a typical VARTM infiltration described in reference (7). The vacuum bag was initially evacuated to 0.5 in Hg (1.7 kPa compaction pressure) to zero the LVDT. For the dry preform test, the vacuum bag was then steadily evacuated to full vacuum (101 kPa compaction pressure). Once the preform displacement stabilized, the bag was steadily vented back to 0.5 in Hg.

For the wet preform test, the bagged preform was initially impregnated with wetting fluid by applying a small pressure gradient to the preform. Once the preform was fully impregnated, full vacuum was applied to the bag until a steady state compaction deformation was measured. Then, the bag was slowly vented by opening the inlet and allowing resin to flow back into the preform. The results are displayed in the next section.

4.2 Permeability Experiments were conducted to characterize the in-plane (S_{xx} and S_{yy}) and the through-thickness (S_{zz}) permeability at fiber volumes ranging from 45% to 58%. The tests were performed at or below the VARTM injection pressure of 101 kPa. Side-view schematic diagrams of the in-plane and through-thickness permeability test fixtures are shown in Figure 2-A) and B). Both the in-plane and through-thickness fixtures were essentially rigid steel molds instrumented with diaphragm pressure sensors and LVDTs. The fixtures were mounted in a compression test frame. The in-plane fixture was designed to characterize preform specimens 15 cm x 15.3 cm at thicknesses ranging from 0.2 cm to 2.5 cm.

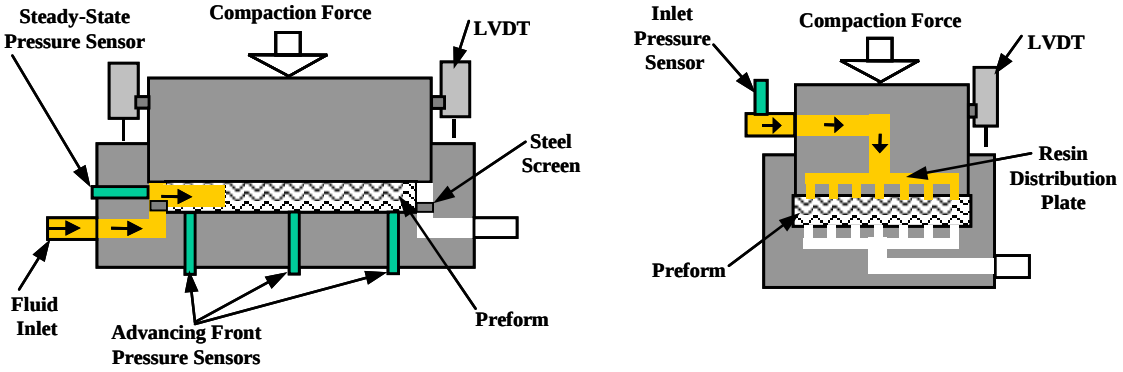

A) In-plane fixture B) Through-thickness fixture

Figure 1 In-plane and through-thickness permeability fixtures.

The low-end thickness limit was due to the thickness of a strip of steel mesh placed at either end of the preform. The mesh was added to the fixture after initial tests at the lower fiber volumes showed that the preform specimens were sliding across the ground surface of the fixture. The mesh was placed on both ends of the preform to ensure identical boundary conditions at both the resin filling and exiting sides. The in-plane fixture utilized two LVDTs to ensure uniform thickness across the 15.0 cm length of the specimen. Four pressure sensors were contained in this fixture. The sensor located at the inlet side was utilized in this study for permeability characterization under steady-state conditions. The remaining three pressure sensors can be used for advancing-front characterization. In testing the MAWK fabric, the specimen was placed so that the 0° rovings were length-wise, or parallel to the direction of resin flow for determination of S_{xx} permeability. For S_{yy}, the specimen was placed so that the 0° rovings were perpendicular to the direction of flow. The through-thickness, S_{zz}, fixture (Figure 2B) was designed to test fabric specimens 5.08 cm x 5.08 cm up to 3.20 cm thick. The concept is identical to that of the in-plane fixture except that the fluid flowed into and out of the specimen via a rigid distribution plunger and base plates, which rested against the 25.81 cm^2 surface on both sides of the specimen. The plate contained a hole-pattern with 0.50 cm holes drilled every 0.64 cm.

NATIONAL INSTRUMENTS® data acquisition hardware and LABVIEW® software are used to record the pressure difference (inlet and outlet), ΔP, mass flow rate, M, and thickness, t. The fiber volume fraction, Vf, is calculated according to Equation 4:

$$V_f = \frac{FAW}{t * \rho_F} \qquad [4]$$

where FAW is the fiber areal weight of the preform specimen and ρ_F is the density of the fabric.

The superficial or filter velocity, q, is calculated according to Equation 5.

$$q = \frac{M}{\rho_R A} \qquad [5]$$

ρ_R is the density of the fluid and A is the cross-sectional area of the preform normal to the flow. The permeability constant, S, is then calculated at each compaction level by the relation from Darcy's Law:

$$S = \frac{q \eta L}{\Delta P} \qquad [6]$$

where η is the viscosity of the fluid and L is the length of the preform specimen.

5.0 CHARACTERIZATION RESULTS

5.1 Compaction In Figure 3 a typical compaction test data set is shown for four stacks of the MAWK fabric including dry compaction, dry unloading and wet unloading modes. The independent variable "Pressure" is plotted on the ordinate to provide ease of view. The fiber lubrication is noted by the increase in fiber volume fraction at 101 kPa after the fabric specimen is wetted. The wet unloading portion of the curve is a quasi-static representation of the infusion of the fabric during a VARTM infiltration. The hysteresis phenomenon is evidenced by the difference in the starting point of the dry compaction curve at Vf = 47% and the ending point of the dry unloading curve at Vf = 52%. This difference of 5% represents the permanent or inelastic deformation of the fabric. The region of the dry unloading curves from Vf = 55% to 52% represents the elastic response of the fabric.

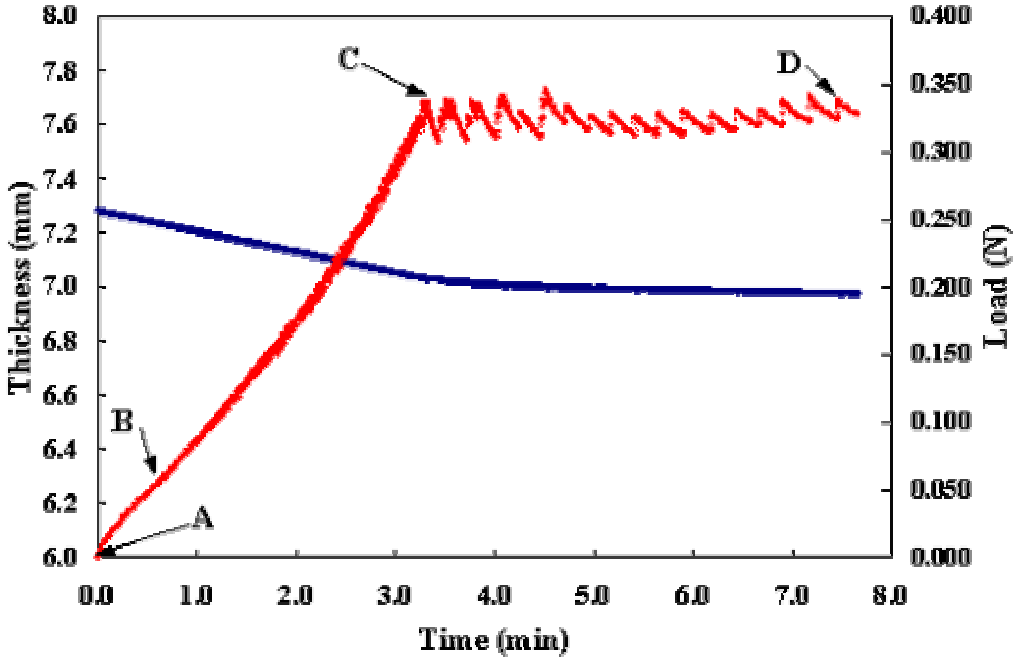

Figure 2 Initial thickness determination performed in test frame.

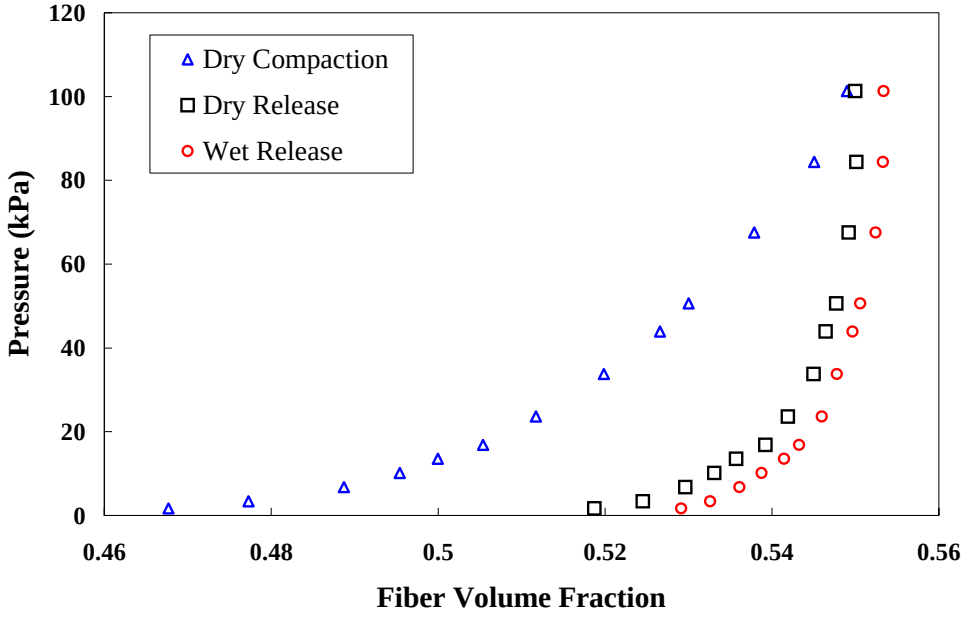

Figure 3 Compaction behavior of MAWK fabric in dry and wet conditions.

Since no general constitutive model is available to describe the compaction behavior of this type of preform, the relationship between the compressive strain in the preform and the applied

pressure is obtained by fitting the compaction curve data to an empirical model. Equation 7 shows the relationship between the fiber volume fraction, Vf and the strain, ε, where ϕ is the initial preform porosity.

$$V_f = \frac{1-\phi}{1-\varepsilon} \qquad [7]$$

Prior to a VARTM infusion the fiber preform is compacted beneath the vacuum bag. Thus, the compressive strain of the preform can be calculated by curve fitting to the dry compaction results. As the flow front moves thru the preform, thus wetting the fabric, the local net pressure applied to the preform decreases according to Equation 1. Therefore the strain in the wet preform is determined by fitting an empirical model to the wet unloading test results. The resulting equations were fit to data from four dry-compaction and wet-unloading tests:

$$\varepsilon_{dry} = a_{dry}(1 - e^{(b_{dry} * P_f)}) \qquad [8]$$

$$\varepsilon_{wet} = a_{wet} + b_{wet}(\frac{P_f}{c_{wet} + P_f}) \qquad [9]$$

where P_f is the net pressure applied to the preform and the averaged constants for four samples are given in Table 2 below.

Table 2 Compaction Model Parameters.

	Constant	**Value**
Dry Compressive Strain, ε_{dry}	Max strain (at P_f = 101kPa), a_{dry}	0.151
	Curve fit constant, b_{dry}	-0.034
Wet Compressive Strain, ε_{wet}	Min strain (at Pf = 10kPa), a_{wet}	0.122
	Curve fit constant, b_{wet}	0.035
	Curve fit constant, c_{wet}	14.076

The results of the dry and wet compaction model equations as well as the statistical deviation are plotted in Figure 4.

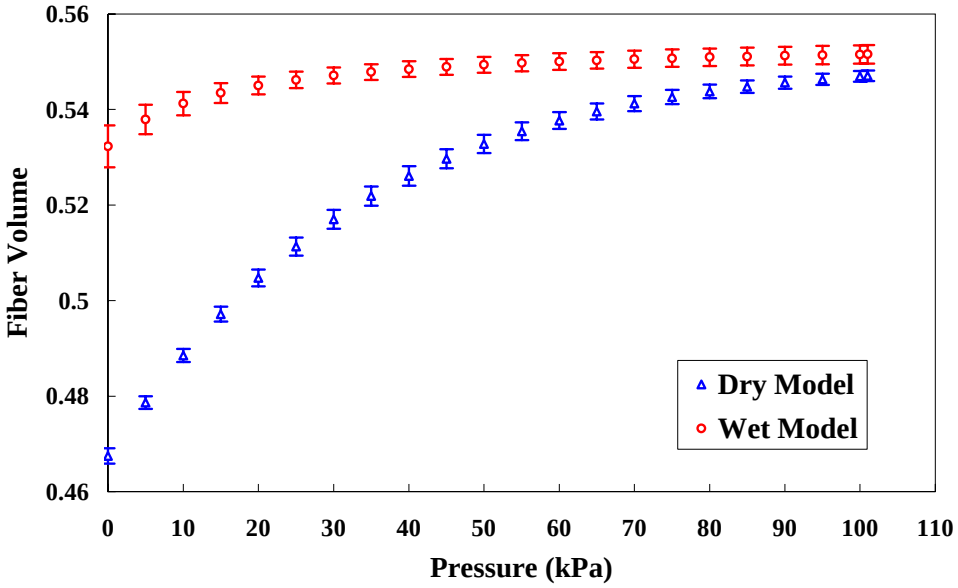

Figure 4 Resulting curves and error from dry and wet compaction model equations.

5.2 Permeability A power law equation was used to fit the permeability data as a function of the fiber volume fraction:

$$S = a(V_f)^b \qquad [10]$$

where S is the permeability in m^2, V_f is the fiber volume fraction and a and b are the empirical constants. Table 3 shows the constants obtained from fitting Equation 10 to the measured experimental data. Figure 5 shows the comparison between the permeability model and the measure data. The resulting transverse, S_{zz}, permeabiltiy constant values are signficantly lower than those found for the in-plane directions.

Table 3 Permeability model empirical constants.

	a	**b**
In-plane, parallel to knitting, Sxx	2.97×10^{-13}	-6.58
In-plane, normal to knitting, Syy	1.53×10^{-12}	-4.24
Through the thickness, Szz	3.56×10^{-15}	-8.64

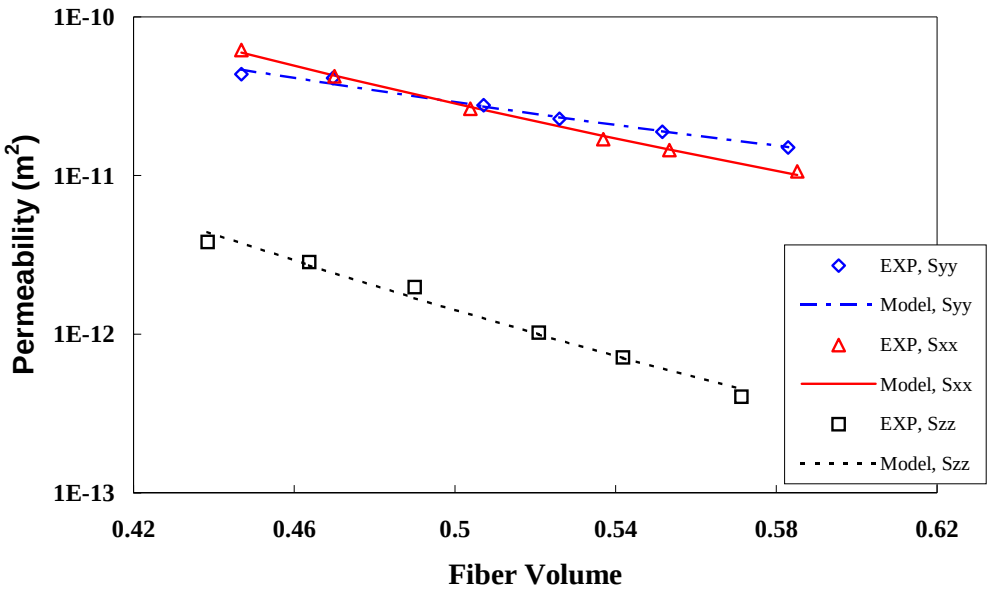

Figure 5 Permeability experimental and model curves for four stacks of MAWK fabric.

Both the permeability and compaction empirical models were implemented in the finite element code 3DINFIL as part of the material database.

6.0 FINITE ELEMENT SIMULATIONS

The process model 3DINFIL was originally developed for RTM to simulate the flow of a resin through a three-dimensional anisotropic preform. The resin is assumed to be an incompressable, Newtonian fluid. The governing differential equation for flow is based on Darcy's law and solved using the Finite Element / Control Volume (FE/CV) technique. The FE/CV method eliminates the need for remeshing of the resin-filled domain for each time step, thus the flow simulation can be performed rapidly and efficiently. Song et.al.(6) modified the existing model to account for the variation in fiber volume fraction during VARTM infiltration due to the flexible tooling and varying pressure inside the mold cavity. The new model 3DINFIL-5.0 features a numerical compaction sub-model, which is coupled to the existing Darcy flow model. At each time step, the resin pressure distribution is obtained from the flow model and the pressure supported by the preform is computed using Equation 1, listed previously. The transverse strain is then calculated using the relations developed in the empical compaction models Equations 8 and 9. The resulting values for strain are converted to fiber volume fraction using Equation 7. The result are input back to the flow model. The fluid velocity is then calculated using Darcy's law and the empirical equations developed for permeabilty, Equation 10.

In this work proceeding two-dimensional simulations of a flat preform are conducted with the empirical models developed in this study for compaction and permeability. The panel contained four stacks of MAWK fabric having dimensions of 30.0 cm x 60.0 cm. The initial porosity value of 0.532 used in the simulations was computed from the thickness value found in the load frame

compaction test. The in-plane and transverse permeability values used for the distribution media were 8.31×10^{-9} m^2 and 5.49×10^{-10} m^2, respectively. Figure 6 depicts the geometry and boundary conditions used in the simulations. In the first simulation the resin was supplied to the panel as a point source and a single node was flagged as saturated with resin pressure of 101 kPa. In the second simulation the resin was supplied as a line source and hence all of the nodes at the resin side boundary were saturated. In both cases the medium was located 2.54 cm from the vacuum side of the panel.

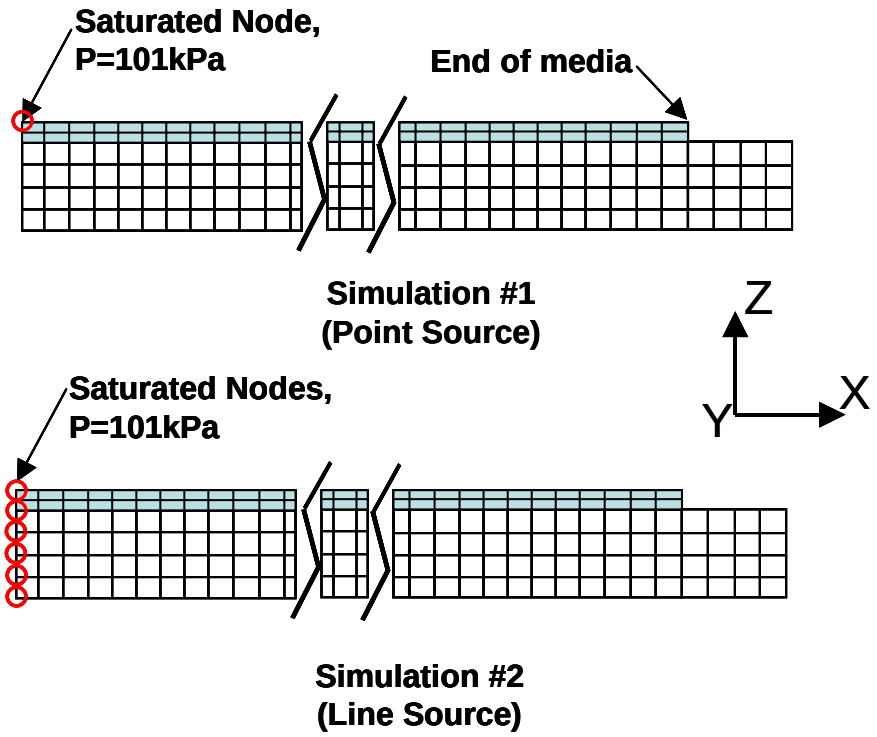

Figure 6 Finite element model geometry and boundary conditions.

The results of the simulations are compared to a glass tool infiltration experiment conducted using four stacks of the MAWK fabric cut to identical dimensions as those in the model geometry. The preform was infiltrated using the same fluid (oil) that was used in both the wet compaction and permeability characterization. The viscosity measured at the time of the infiltration was input to the model.

Good agreement was obtained between the simulations and the experiment for the flow front evolution at the top and the bottom of the preform. The point-source boundary condition used in Simulation #1 resulted in a closer prediction of the final fill time for both the top and bottom surface, however this model did not capture the beginning of the curve on the bottom side. Observations of the actual flow in the panel indicate that there is initially a small amount of in-plane flow on the bottom surface of the resin side. At approximately 40 seconds into the infiltration, the in-plane flow becomes dominated by flow in the transverse. Future work will involve further investigation of how specifically the placement of the resin source influences the model predictions.

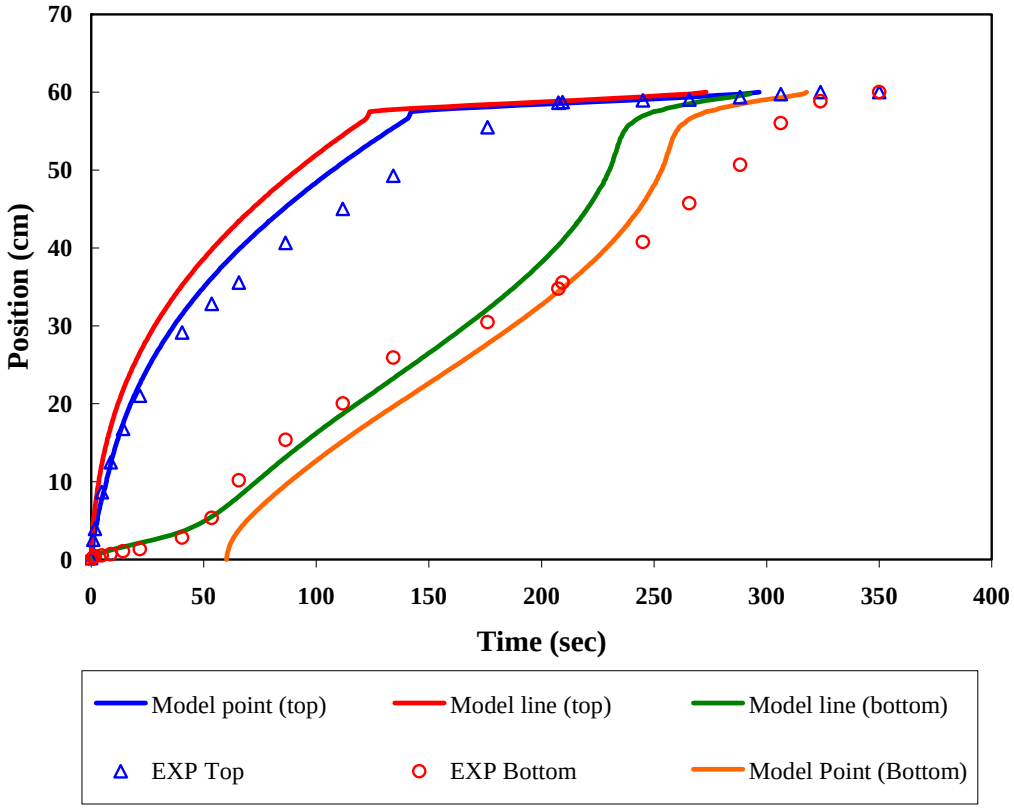

Figure 7 Finite element model simulation results and glass tool infiltration experiment data.

7.0 CONCLUSIONS

The development and use of a finite element process model plays a key role in developing a complete understanding and therefore fully maximizing the potential of the VARTM process. Unlike the well characterized RTM process, a method to accurately predict flow in VARTM infiltration has not been developed in any sense that is widely accepted. This work focused on the development of more accurate empirical models to characterize the compaction behavior and permeability of a non-crimp, multi-axial carbon fabric. A new method to measure the initial thickness of the preformed was employed. The resulting compaction model equations fit the data well and showed little variability for different test samples. The preform permeability and compaction models were incorporated in the 3DINFIL process model. The resulting simulations accurately predicted the flow front evolution measured for a four stack thick panel of MAWK fabric.

8.0 REFERENCES

1 . L.R. Thomas, A.K. Miller and A.L. Chan, SAMPE International Symposium, 47, 570, (2002).

2 . J. M. Criss, S.C Parsons and R.W. Koon, SAMPE International Symposium, 49, 1049, (2004).

3 . W.H. Seemann, (1990), U.S. Patent 4,902,215.

4 . W.H. Seemann, (1994), U.S. Patent 5,316,462.

5 . G. Fernlund, A. Poursartip, K. Nelson, M. Wilenski and F. Swanstrom, SAMPE International Symposium, 44, 1744, (1999).

6 . X. Song, "Vacuum Assisted Resin Transfer Modeling (VARTM): Model Development and Verification", Ph.D. Dissertation, Department of Engineering Science and Mechanics, Virginia Polytechnic Institute and State University, Blacksburg, VA, (2003).

7 . B.W. Grimsley, P. Hubert, X. Song, R.J. Cano, A.C. Loos and R.B. Pipes, SAMPE International Technical Conference, 33, 140, (2001).

8 . A. Hammami, Polymer Composites, 22, (3), 337, (2001).

9 . M. Andersson, S. Lundstrom, B.R. Gebart and R. Langstrom, 8th International Conference on Fiber Reinforced Composites, 113, (2000).

10 . A. Somasheka, S. Bickerton, D. Battacharyya, 7th International Conference on Flow Processes in Composite Materials, , 425, (2004).

11 . T. Kruckenberg and R. Paton, 7th International Conference on Flow Processes in Composite Materials, 418, (2004).

12 . A.C. Loos, J.R. Sayre, R.D. McGrane and B.W. Grimsley, SAMPE International Symposium, 46, 1049, (2001).

13 . T. Sadiq, R. Parnas and S. Advani, International SAMPE Technical Conference, 24, 674, (1992).

14 . B.W. Grimsley, R.J. Cano, B.J. Jensen, A.C. Loos and P. Hubert, 18th Annual Technical Conference of the American Society of Composite, (2003).